Revue Roumaine de Chimie, **2008**, *53*(6), 471–479

THE EFFECT OF SURFACE ACTIVE COMPOUND ADSORPTION ON FREE DROP DEFORMATIONS

Ioan-Răducan STAN,[a] Maria TOMOAIA-COTISEL[b,*], Aurelia STAN[c] and Cristina BORZAN[d]

[a]Babes-Bolyai University of Cluj-Napoca, Faculty of Mathematics, Department of Mechanics and Astronomy, 1 Kogalniceanu Str., 400084 Cluj-Napoca, Roumania
[b]Babes-Bolyai University of Cluj-Napoca, Faculty of Chemistry and Chemical Engineering, Department of Physical Chemistry, 11 Arany Janos Str., 400028 Cluj-Napoca, Roumania
[c]Augustin Maior Technical College, 78 Calea Motilor Str., 400370 Cluj-Napoca, Roumania
[d] Iuliu Haţieganu University of Medicine and Pharmacy, Department of Public Health and Management, 13 Emil Isac Str., 400023 Cluj-Napoca, Roumania

Received January 23, 2007

The effect of the surface active compound adsorption on the surface of a free liquid drop immersed in an unbounded liquid (the densities of the two bulk liquids are equal) is studied. The variation of the interfacial tension gives rise to a surface flow (*i.e.* Marangoni flow) which causes the motion of the neighboring liquids by viscous traction, and generates a hydrodynamic pressure force (named Marangoni force) which acts on the drop surface. The Marangoni force is the principal force that develops the deformations of the free drop, while the capillary forces, the surface dilution and the tip-stretching are secondary factors. The observed experimental data are in a substantial agreement with the results of our theoretical hydrodynamic model.

INTRODUCTION

In attempts to describe the movements and deformations of a free liquid drop, immersed in an equal density bulk liquid, when a surface tension gradient is applied on the drop surface, some theoretical models and experiments were developed to explain the drop dynamics.[1-6] It was suggested that Marangoni instability, surface dilution, tip-stretching and capillary forces are important factors in drop movements and deformations.

To determine which one from these is a major factor on the drop dynamics, in this work, we investigate experimentally and theoretically the effect of local changes in the surface tension, which are induced by the adsorption of a surfactant at the drop surface.

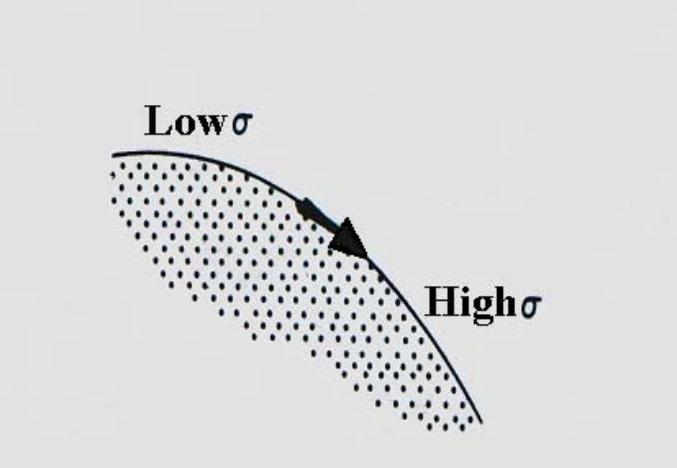

Fig. 1 – Interfacial Marangoni flow (see, the arrow) caused by a surface tension gradient.

* Corresponding author: mcotisel@yahoo.com

As a result of the adsorption of a surfactant (which is a term used interchangeable with surface active compound) a surface tension gradient (Marangoni effect) appears, which generates a real surface flow, called the Marangoni flow, and it is illustrated in Fig. 1. This surface Marangoni flow causes the motion of the neighboring liquids by viscous traction,[5, 6] and generates the force of hydrodynamic pressure, named Marangoni force, which acts on the drop surface.

Also, in this work, we have developed a theoretical hydrodynamic model to calculate the Marangoni force. This force acts like a "hammer" and modifies the shape of the drop. This force also generates other various factors, like the surface dilution, the tip-stretching, and the capillary forces, that might appear in the drop dynamics, depending on the working conditions. The results of our theoretical hydrodynamic model are in a substantial agreement with the observed experimental data.

THEORY

The investigation of the free drop dynamics is of a present interest, due to its appearance both in the industrial and biological processes, as well as in the space science and technology of liquids.

Hydrodynamic model

We consider a viscous (L') liquid drop (with density ρ') immersed in an unbounded immiscible (L) liquid (of density ρ) at a constant temperature (T). The densities of the two bulk liquids are equal (ρ = ρ') and initially the drop is motionless. Such a drop is also called free drop.

Further, we assume that both liquids (L and L') are incompressible and Newtonian. The drop has a viscosity μ' and the surrounding bulk fluid a viscosity μ, which are, in general, different. The surface between the two bulk fluids is caracterized by an interfacial tension noted σ_0.

Then, a small quantity of a surfactant (*e.g.* a droplet of 10^{-3}-10^{-2} cm^3, which is very small compared with the volume of the initial drop) is introduced on a well-chosen point (called also injection point) at the drop surface. The surfactant, because of its molecular structure, is spread and simultaneously adsorbed at the liquid-liquid interface and it is continuously swept along the meridians of the drop by the convective transport (see, Fig. 2). In the injection point the interfacial tension is instantaneously lowered to σ_1 value. We mention that local changes in temperature[7-9] and in electric charge or the presence of surface chemical reactions might produce a similar effect.

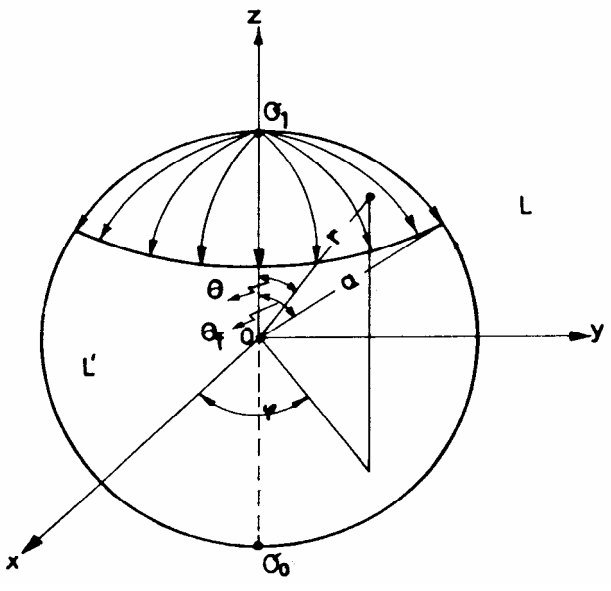

Fig. 2 – The surfactant spreading and adsorption on the drop surface. Marangoni flow at a spherical liquid/liquid interface. The system of spherical coordinates (r, θ, φ); the drop radius is noted *a*; the θ_f angle characterizes the position of the surfactant front. For symbols see the text.

Since the interfacial tension is a function of the surfactant concentration, a gradient of interfacial tension is established over the surface of the drop.[10] Consequently, the Marangoni spreading of the surfactant takes place from low surface tension to high surface tension (Fig. 1). As a result of the

Marangoni surface flow, which causes the motion of the neighboring liquids by viscous traction, the Marangoni force of hydrodynamic pressure will appear acting on the drop surface. Due to the drop symmetry, the Marangoni force has the application point in the injection point with surfactant at the drop surface.

This Marangoni force will determine all kinds of drop movements, especially deformations, rotations and oscillations of the whole drop, as well as surface waves and drop translational motions depending on the experimental working conditions.

The symmetry of the problem suggests a system of spherical coordinates (r, θ, φ) with the origin placed in the drop center and with the Oz axis passing through the sphere in the point of the minimum interfacial tension, *i.e.* the injection point of the surfactant.

We underline that the surfactant injection point at the drop surface may be taken anywhere, the drop being initially at rest. In the following, we shall take it like shown in Fig. 2. The surfactant front position, in this radial flow, is noted by the angle θ_f. The interfacial tension, σ, is considered a unique function of the angle θ. Within the surfactant invaded region, $(0 \le \theta \le \theta_f)$, for the variation of the interfacial tension[6] with θ, we take:

$$\sigma(\theta) = \frac{\sigma_0 - \sigma_1}{1-\cos\theta_f}(1-\cos\theta) + \sigma_1 \qquad (1)$$

where $\sigma_0 = \sigma(\theta_f)$ and $\sigma_1 = \sigma(0)$.

Derivation of Eq. (1) gives the interfacial tension gradient in the invaded drop region with surfactant

$$\frac{d\sigma}{d\theta} = \frac{\sigma_0 - \sigma_1}{1-\cos\theta_f}\sin\theta \qquad (2)$$

where, the interfacial tension σ_0 is constant in any point of the uncovered surface, while the interfacial tension difference $\Pi = \sigma_0 - \sigma_1$ arises only in the invaded region. It is clear that only σ_1 and σ_0, i. e. the minimum and the maximum values of the interfacial tension, can be experimentally measured. The equations governing the flow inside and outside the drop are the continuity and Navier-Stokes equations.[11-13]

The continuity equations for an incompressible fluid are

$$\text{div } \vec{v} = 0, \qquad (3)$$

$$\text{div } \vec{v}' = 0, \qquad (4)$$

where $\vec{v}$ is the velocity of the bulk liquid L and $\vec{v}$' the velocity of the liquid L' within the drop.

The Navier-Stokes equations for a steady flow are:

$$(\vec{v}\cdot\nabla)\vec{v} = -\frac{1}{\rho}\text{grad } p + \nu\Delta\vec{v} \qquad (5)$$

$$(\vec{v}'\cdot\nabla)\vec{v}' = -\frac{1}{\rho}\text{grad } p' + \nu'\Delta\vec{v}' \qquad (6)$$

where p and p' are the pressures outside and inside of the drop; $\nu = \frac{\mu}{\rho}$ and $\nu' = \frac{\mu'}{\rho}$ are the kinematic viscosities of continuous liquid and drop liquid, respectively. All these parameters are considered constants.

The drop surface is considered a two dimensional, incompressible Newtonian fluid, and the equation of the interfacial flow[14-16] is given by:

$$\Gamma\left(\vec{w}\cdot\nabla_S\right)\vec{w} = \vec{F} + \nabla_S\sigma + (\kappa+\varepsilon)\nabla_S\left(\nabla_S\cdot\vec{w}\right) \qquad (7)$$

where $\vec{w} = \vec{v}_s$ is the interface velocity, $\vec{F} = \Gamma\vec{g} + \vec{T} - \vec{T}'$ is the external force acting on the drop surface, $\vec{T}$ and $\vec{T}'$ are the tractions exerted by the outer and inner liquid on the drop interface, Γ is the surface density, κ and ε are the surface dilatational and shear viscosity, respectively, and ∇_S is the surface gradient operator. Because the surface density[16] is very small ($\Gamma \approx 10^{-7}$ g cm^{-2}) the inertial term can be neglected against the remainder terms.

Eqs. (3-7) with the appropriate boundary conditions[11-13] lead to the distribution of the velocities $\vec{v}, \vec{v}'$ and of the pressures p, p' outside and inside the drop:[17]

$$v_r(r,\theta) = \frac{(\sigma_0-\sigma_1)a^3}{3(\mu+\mu'+2\kappa/3a)(1-\cos\theta_f)}\left(\frac{1}{r^3}-\frac{1}{a^2r}\right)\cos\theta \qquad (8a)$$

$$v_\theta(r,\theta) = \frac{(\sigma_0-\sigma_1)a^3}{3(\mu+\mu'+2\kappa/3a)(1-\cos\theta_f)}\left(\frac{1}{2r^3}+\frac{1}{2a^2r}\right)\sin\theta \qquad (8b)$$

$$p(r,\theta) = -\frac{\mu(\sigma_0 - \sigma_1)a}{3r^2(\mu + \mu' + 2\kappa/3a)(1-\cos\theta_f)}\cos\theta \tag{8c}$$

for the outer flow, and

$$v_r'(r,\theta) = \frac{\sigma_0 - \sigma_1}{3(\mu + \mu' + 2\kappa/3a)(1-\cos\theta_f)}\left(1 - \frac{r^2}{a^2}\right)\cos\theta \tag{9a}$$

$$v_\theta'(r,\theta) = -\frac{\sigma_0 - \sigma_1}{3(\mu + \mu' + 2\kappa/3a)(1-\cos\theta_f)}\left(1 - \frac{2r^2}{a^2}\right)\sin\theta \tag{9b}$$

$$p'(r,\theta) = -\frac{10\,\mu'(\sigma_0 - \sigma_1)r}{3\,a^2(\mu + \mu' + 2\kappa/3a)(1-\cos\theta_f)}\cos\theta \tag{9c}$$

for the inner flow.

Marangoni force F_M exerted on the free drop

Further, we describe the Marangoni force exerted on the free drop due to Marangoni flow. This force F_M, due to the symmetry of the Marangoni flow, is oriented along the Oz axis and has been computed by integrating the surface forces[11] acting along the drop surface:

$$F_M = \iint_S (p_{rr}\cos\theta - p_{r\theta}\sin\theta)\, ds \quad , \tag{10}$$

where, ds is the surface element covered with surfactant, and p_{rr} and $p_{r\theta}$ are the normal and tangential components,[11-13] respectively, of the viscous stress tensor:

$$p_{rr}(r,\theta) = -p + 2\mu\frac{\partial v_r}{\partial r} \tag{11}$$

$$p_{r\theta}(r,\theta) = \mu\left(\frac{1}{r}\frac{\partial v_r}{\partial \theta} + \frac{\partial v_\theta}{\partial r} - \frac{v_\theta}{r}\right) \tag{12}$$

The surface element in spherical coordinates on the drop (*e.g.*, drop radius, r = a) is

$$ds = 2\pi a^2 \sin\theta\, d\theta$$

and, the force acting on the drop, given by (Eq. (10), can than be rewritten as:

$$F_M(\theta_f) = 2\pi a^2 \int_0^{\theta_f} (p_{rr}\cos\theta - p_{r\theta}\sin\theta)\sin\theta\, d\theta\,. \tag{13}$$

From Eqs. (8) one obtains for the normal (Eq. (11)) and tangential components (Eq. (12)) of the stress tensor, at the drop surface (r = a):

$$(p_{rr})_{r=a} = -\frac{\mu(\sigma_0 - \sigma_1)}{a(\mu + \mu' + 2\kappa/3a)(1-\cos\theta_f)}\cos\theta\,, \tag{14}$$

$$(p_{r\theta})_{r=a} = -\frac{\mu(\sigma_0 - \sigma_1)}{a(\mu + \mu' + 2\kappa/3a)(1-\cos\theta_f)}\sin\theta\,. \tag{15}$$

Introducing the viscosities ratio, $\lambda = \mu'/\mu$, the interfacial tension difference, $\Pi = \sigma_0 - \sigma_1$, and because $2\kappa/3a \approx 0$ as shown previously[5] we have after integration:

$$F_M(\theta_f) = \frac{2\pi\, a\,\Pi}{3(1+\lambda)}(1 - 2\cos\theta_f - 2\cos^2\theta_f) \tag{16}$$

Thus, Eq. (16) represents the Marangoni force (noted F_M) acting on the drop surface along the Oz axis. It can be seen that this force depends on the θ_f angle, namely, on the extent to which the drop surface is covered by the surfactant, as a function of the radial interfacial tension difference (Π), the ratio of the bulk viscosities (λ), as well as of the radius (a) of the drop.

The value of θ_f, for which the force cancels F_M (θ_f) = 0, is $\theta_0 = 68.53^0$. We emphasize that for $\theta_f \in [0, \theta_0)$, the force is negative $F_M(\theta_f) < 0$, and for $\theta_f \in (\theta_0, 180^0]$ the force is positive $F_M(\theta_f) > 0$, having the greatest value for $\theta_m = 120^0$.

It means that for a coverage degree of the drop surface with surfactant for $\theta_f < \theta_0$, the Marangoni force F_M exerted on the drop is oriented toward the negative direction on the Oz axis. This situation is similar with the application of a "hammer" knock on the drop surface in the injection point of the surfactant.

For a coverage degree θ_f greater than θ_0, but less than 180^0, the force $F_M(\theta_f)$ is oriented towards the positive direction of the Oz axis. It is also named the propulsive (lifting) force, as suggested earlier,[1-6, 11] responsible for the translational movement of the drop, which appears only when the coverage of the drop with surfactant is greater than θ_0.

Therefore, the effect of the surface coverage with surfactant at the drop surface can be decomposed into two parts: (*i*) the "hammer" effect for the coverage of $0 \le \theta_f < \theta_0$ when the drop is practically motionless and (*ii*) the "propulsive " effect for the coverage of $\theta_0 < \theta_f \le 180^0$ responsible for the upward movement of the drop.

An important observation is that the action of the Marangoni force $F_M(\theta_f)$ is maximum at the injection point of the surfactant, for which $\theta_f = 0$. For physical meanings, we take the absolute value of Marangoni force, $|F_M(0)|$, noted $F_M(0)$. Therefore, for $\theta_f = 0$, the Eq. (16) becomes:

$$F_M(0) = \frac{2 \pi a \Pi}{1 + \lambda} \quad . \qquad (17)$$

Further, we suggest that it is a direct connection between Marangoni force, $F_M(0)$, and the deformation of the drop.[17,18] The modification of the surface area of a drop, when the drop is deformed to a nonspherical shape, dilutes the surfactant surface concentration and the deformation of the drop is a complex process. This is called the surface dilution effect. Also, surface active molecules may accumulate at the tip of the drop due to convection, especially at the break-up process of the drop. This decreases the local interfacial tension and causes the tip to be overstretched. This is called the tip-stretched effect.

When during the deformations, a drop gets a concave surface, capillary forces appear which tend to bring the drop in the initial spherical shape.[19-23] All deformations appear only as a consequence of the hammer effect and convective flow of the surface active molecules. Clearly, it is a direct connection between Marangoni force and drop deformations via the surface waves produced by the hammer effect, as recently revealed.[17,18] Moreover, the surface waves, generated by the hammer effect, produce traveling periodic internal wave trains. If these internal waves are absorbed by the drop, the shape of the drop is not deformed (Fig. 2). If these internal waves are not absorbed, the overlapping of the direct and reflected internal waves modifies the shape of the drop and causes various deformations or even the break-up of the drop.

Therefore, we suggest that the primary effect, due to a reduction of the equilibrium interfacial tension (σ_0) in the injection point of a free drop surface with a surfactant, at t=0, is the appearance of a real surface flow (*i.e.* Marangoni flow) of the surfactant on the drop surface. This convection flow of the surfactant modify the equilibrium surface tension, σ_0, and the Marangoni force, $F_M(0)$, which acts like a hammer, appears. This force changes the shape of the drop, and consequently, several factors might be generated, namely, the surface dilution and tip-stretching, as well as capillary forces.

EXPERIMENTAL

The experimental work on drop dynamics and Marangoni instability was performed in liquid-liquid systems of equal densities presented in Tables 1 and 2.

The densities of the liquids were determined picnometrically and the bulk viscosities by using an Ubbelhode viscometer. The surface dilatation viscosity at the liquid/liquid interface was not directly measured and only a few indications concerning this magnitude for the liquid/gas interface have been reported.[4] The interfacial tension of the liquid/liquid systems was determined by a method based on capillarity[4] and its value is given in Table 1. The measurement of the above parameters as well as the drop dynamics and surface flow experiments have been performed at constant temperature (20 ± 0.1 ^oC). All chemicals were of analytical purity and used without further purification.

The mixtures making up the continuous L phase were placed in a thermostated parallelepiped vessel of 1 dm^3, made of transparent glass. The drop was made of various radii between 0.46 and 1.19 cm, using the mixtures described in Table 1. The L' liquid was carefully submerged by using a pipette into the continuous L aqueous phase and the density of the latter was then adjusted by adding small quantities of water or alcohol until the buoyancy of the drop practically disappeared.

After the system was stabilized, a small quantity (10^{-3}-10^{-2} cm^3) of the surfactant solution was injected with a micrometric syringe, in a point on the drop surface (injection point in Fig, 2). The injection was done either in a vertical

direction (as in Fig. 3) or in different directions (Figs 4 and 5) and no influence of the mode of injection on the Marangoni flow or on drop movements and deformations were observed.

In order to make visible the surface flow, the surfactant solution was intensely colored with methylene blue (0.28 g/100 cm^3). We mention that we used surface active compounds which were soluble in the continuous phase L for systems 1 and 2. For systems 3 to 6, the surfactant was insoluble in both liquid L and L' phases.

The movement of the surfactant front was followed with a high speed camera (500 images/sec). A number of sequences showing the surfactant front position at various moments t of the process is presented in Fig. 3. It can be seen that the front position is easily distinguishable from the uncovered drop surface.

The positioning of the L' drop in the continuous L liquid for a sufficiently long time as to perform the flow measurements raises difficulties. Although, some authors pointed out that two drops never behave in the same manner under the action of interfacial tension differences, we have succeeded in measuring the surface flow velocities[4] and here, in determining the influence of several factors, like interfacial tension gradients, viscosities, on the drop deformations and movements.

RESULTS AND DISCUSSION

Drop deformations

In Table 1, we give the experimental parameters for three different cases of drop dynamics, under various surface tension gradients Π. The first case (systems 1 and 2) corresponds to the undeformable drops (Fig. 3). The second one (systems 3 and 4) represents the case of deformable drops (Fig. 4) and the third one (Fig. 5) describes the deformation and the break-up of a drop (systems 5 and 6). Also, Table 1 gives the composition of the continuous (L) bulk and drop (L') liquid phases, as well as the description of the surface active compound phase and various phase physical characteristics. The continuous liquid bulk phase (μ) and drop phase (μ') viscosities and the interfacial tension, σ_0 and σ_1, values are also given in Table 1. Investigated drops have the radius comprised between 0.46 and 1.19 cm.

Table 2 gives the values of the surface tension gradient, $\Pi = \sigma_0 - \sigma_1$, the ratio of the bulk viscosities $\lambda = \mu'/\mu$, the radius of the drops, a, and the calculated Marangoni force $F_M(0)$.

Then, we compare the theoretical values, obtained with our hydrodynamic theoretical model, with some experimental observations on the movements and the deformations of the drops under the surface tension gradient. The movements and the deformations of the drops were followed by filming with a high-speed camera (500 images/sec). Several image sequences illustrating the deformations of the drop at various moments (at different times, t) are presented in Figs. 3-5.

Table 1

Composition and physical characteristics of the liquid/liquid systems of equal densities. For systems 3 to 5, the composition of phase L is given in (% of weight). For bulk viscosities μ and μ', and interfacial tensions σ_0 and σ_1, see the text. For systems 1 and 2, the drop radius is a = 1.19 cm. For systems 3 to 6, the drop radius is a = 0.46 cm

Syst No.	Density g/cm^3	Continuous Phase (L)			Drop Phase (L')		Surfactant Solution	
		Composition (% vol)	μ(cP)	σ_0 (dyn/cm)	Composition (% vol)	μ'(cP)	Composition (% vol)	σ_1 (dyn/cm)
1	0.863	Ethanol 78.6 Water 21.4	2.26	7.9	Paraffin oil	80	Propanol 77.3 Water 22.7	3.5
2	0.863	Methanol 78 Water 22	1.33	10.2	Paraffin oil	80	Propanol 77.3 Water 22.7	3.5
3	1.068	$NaNO_3$ 15.1 Water 84.9	1.10	28.7	Chlor benzene 40 Silicon oil 60	8.04	Benzylic alcohol 89 CCl_4 11	3.6
4	1.068	$NaNO_3$ 15.1 Water 84.9	1.10	28.2	Chlor benzene 50 Silicon oil 50	5.46	Benzylic alcohol 89 CCl_4 11	3.6
5	1.066	$NaNO_3$ 15 Water 85	1.10	25.6	Chlor benzene 85 Silicon oil 15	1.40	Benzylic alcohol 89 CCl_4 11	3.5
6	1.064	$NaNO_3$ 14.9 Water 85.1	1.10	22.8	Chlor benzene 92 Silicon oil 8	1.03	Benzylic alcohol 89 CCl_4 11	3.6

Table 2

Surface tension gradients, $\Pi = \sigma_0 - \sigma_1$, the ratio of the bulk viscosities, $\lambda = \mu'/\mu$, the radius of the drop, a, and the absolute values of the calculated Marangoni force $F_M(0)$

System No.	Π (dyn/cm)	λ	*a* (cm)	$F_M(0)$ (dyn)	Remarks
1	4.4 ± 0.3	35.39	1.19	0.90	The free drop remains undeformable, having, at most, surface waves, as in Fig. 3.
2	6.7 ± 0.3	60.15	1.19	0.81	
3	25.1 ± 0.3	7.31	0.46	8.71	The free drop might have slight or big deformations, but after 0.6-0.8 sec., it returns to its initial form, as in Fig. 4.
4	24.6 ± 0.3	4.96	0.46	11.92	
5	22.1 ± 0.3	1.27	0.46	28.10	The free drop, after 0.3-0.4 sec., breaks up into two drops, as shown in Fig. 5.
6	19.2 ± 0.3	0.94	0.46	28.56	

In Fig. 3, the filmed drop images, at different moments of time (t), are shown for the case of an undeformable free drop, *e.g.* the system 2, which is characterized in Tables 1 and 2. In these images is possible to observe the motion of the surfactant front on the drop surface, easily distinguishable, by the contrast with the uncovered drop surface. Also, in Fig. 3, we can observe that the horizontal line, corresponding for the initial position of the free drop, is almost not modified in time and the drop is not deformed or moved. These findings are in substantial agreement with the data earlier published,[4] for other non-deformable free drops. In this study, for comparison, we have chosen similar experimental conditions given in Table 1, for systems 1 and 2, and therefore, we clearly demonstrated the reproducibility of these experiments. In plus, here, we have calculated the Marangoni force $F_M(0)$, see Table 2.

Fig. 4 shows three different shapes of a deformable free drop (a, b, and c) and the drop movement (c) from the initial position (a, *i.e.* from the shown reference horizontal line). In this case, for the system 4, characterized in Tables 1 and 2, due to the variation of the drop shape, besides the Marangoni force, the surface dilution and capillary forces will appear in the description of drop deformations. A similar situation is found for the system 3 also characterized in Tables 1 and 2.

Fig. 5 illustrates the initial free drop (panel a), the drop deformation (panel b) as well as the drop movement and the break-up (panel c) of the drop into two parts. This is the third case of a deformable drop observed for the system 6 and its detailed characterization is given in Tables 1 and 2.

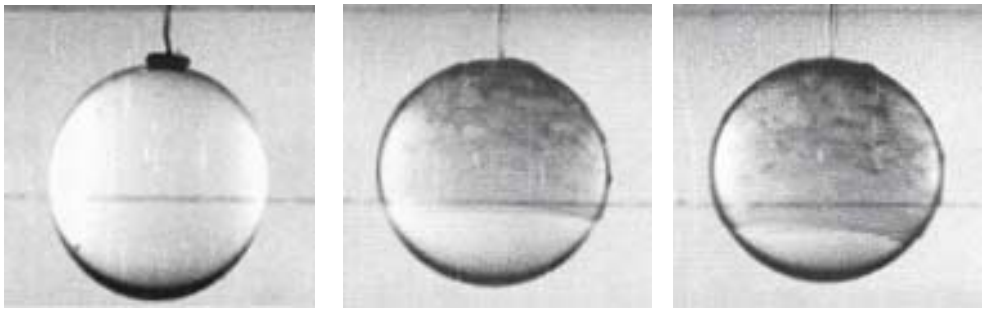

(a) **(b)** **(c)**

Fig. 3 – Filmed pictures of an undeformable drop characterized by the system 2, given in Tables 1 and 2. The interfacial tension difference, $\Pi = \sigma_0 - \sigma_1 = 6.7$ dyn/cm, the viscosities ratio, $\lambda = 60.15$, $F_M(0) = 0.81$ dyn. The time of the surfactant front evolution on the free drop of radius *a* = 1.19 cm, (a) t = 0 sec, (b) t = 1.02 sec, (c) t= 1.25 sec.

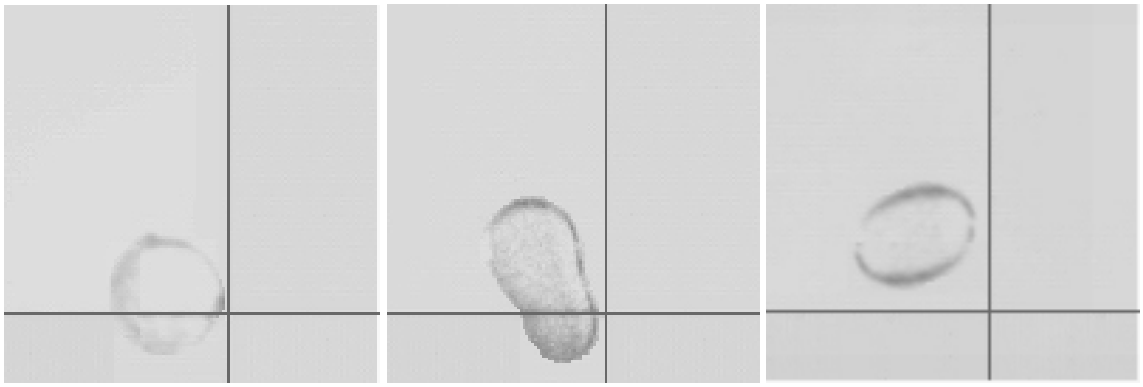

(a) **(b)** **(c)**

Fig. 4 – Filmed pictures of drop deformations. The liquid-liquid system is characterized by the system 4 in Tables 1 and 2; Π =24.6 dyn/cm; λ = 4.96; $F_M(0)$ = 11.92 dyn; (a) t = 0 sec; (b) t = 0.14 sec; (c) t = 0.44 sec; the free drop radius *a* = 0.46 cm. For symbols see the text.

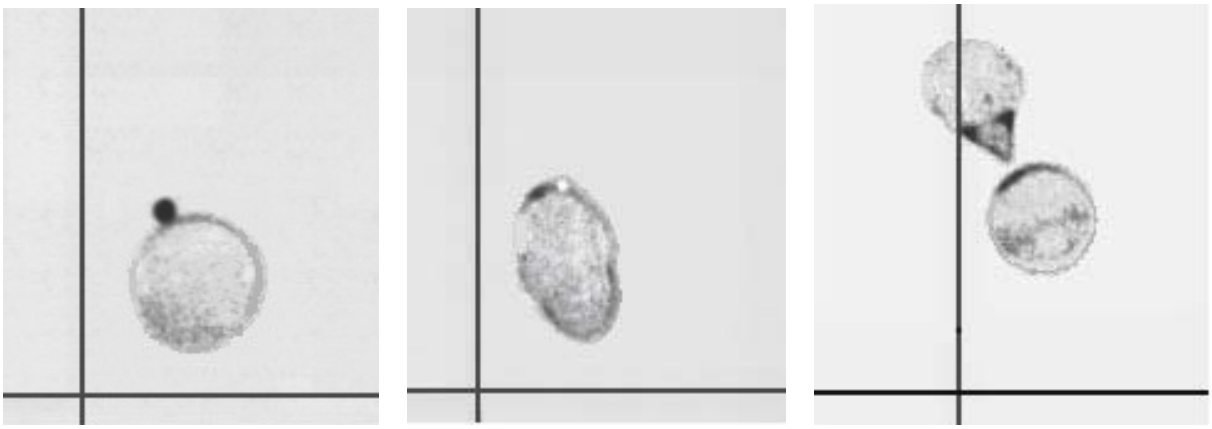

(a) **(b)** **(c)**

Fig. 5– Filmed pictures of the initial free drop (a), the deformed drop (b) and the breakup drop (c). The liquid/liquid system is characterized by the system 6 given in Tables 1 and 2; Π = 19.2 dyn/cm; λ = 0.94; $F_M(0)$ = 28.56 dyn. Time evolution of the drop: (a) t = 0 sec (surfactant injection on drop surface); (b) t = 0.12 sec (drop deformation); (c) t = 0.36 sec (break of the drop); the free drop radius *a* = 0.46 cm. For symbols see the text.

Certainly, it can be seen that at a certain moment in time (Fig. 5, panel c) a tip in one of the drop compartments appears. Fig. 5c might be an example of the tip-stretched effect. This situation is also observed for the system 5, that is characterized in Tables 1 and 2.

As we can see, from Table 2, for systems 1 and 2, the values of viscosities ratio, $\lambda >> 1$, are very large, and the values of the Marangoni force, $|F_M(0)|$, are slightly smaller than 1, and the drop is non deformable (Fig. 3).

For systems 3 and 4, given in Table 1, the ratio values of the bulk viscosities are greater than unity, $\lambda > 1$ (Table 2), and the Marangoni force is much higher than 1. Fig. 4 presents the three different shapes of the free drop dynamics. Because there is a variation of the drop shape, in this second case, the surface dilution and capillary forces will appear. This is the situation of a slightly viscous drop, when the Marangoni effect will provoke the drop deformations, which will generate the surface dilution in parallel with the appearance of capillary forces (Fig. 4b).

For the system 6, described in Tables 1 and 2, the viscosity of continuous bulk (μ) liquid and of the drop (μ') liquid are almost equal, $\lambda \approx 1$ in Table 2, but the Marangoni force has the highest value. In this situation, after a few moments (about 0.36 sec) the break-up of the drop appears (Fig. 5c), and the drop is divided into two parts (droplets). This is the most complicated situation, when the Marangoni force will provoke the drop deformations, which will generate, in parallel, the surface dilution and the tip-stretching, until the drop is broken into two drops, as illustrated in Fig. 5c. This situation is reproducible and it is also

found for the system 5 which is characterized in Tables 1 and 2.

CONCLUSION

A hydrodynamic model has been developed in which the variable interfacial tension at the well defined free drop surface, caused by the addition of an surface active compound, will generate a Marangoni force primarily responsible for the drop deformations and movements.

The drop deformation process is described and analyzed mathematically. It has been shown that it is a deep dependence between the absolute values of the Marangoni force, $|F_M(0)|$, and the deformations of a free drop. In other words, a little Marangoni force will not cause the deformations of the viscous drop, but a large Marangoni force will provoke complicated deformations and movements of a free drop even the break-up of the drop. Thus, it has been shown experimentally and theoretically that the Marangoni force is a primary cause for the deformations of a free liquid drop. Surface dilution and tip-stretching effects, as well as the capillary forces, might appear as secondary factors in the drop deformation processes.

When a surface tension gradient appears at the free drop surface, the magnitude of the hammer Marangoni force determines primarily the drop deformations and movements, taking into account the physical characteristics of the continuous liquid bulk phase and of the drop liquid phase, as well as those for the chosen surfactant solutions as indicated in Tables 1 and 2.

Finally, it is to be emphasized that such phenomena, generated by Marangoni force and Marangoni instability, are a result of the adsorption of a surface active compound at the surface between the two liquid phases. These phenomena are of important interest in industrial, biological, and medical processes, in complex movements at the level of biological membranes, as well as in the space science and technology of liquids.

REFERENCES

1. R. S. Valentine and W. J. Heideger, *Ind. Eng. Chem. Fund.*, **1963**, *2*, 242.
2. R. S. Valentine, N. F. Sather and W. J. Heideger, *Chem. Eng. Sci.,* **1965**, *20*, 719.
3. E. Chifu and I. Stan**,** *Rev. Roum. Chim.,* **1980**, *25*, 1449.
4. E.Chifu, I. Stan**,** Z. Finta and E. Gavrila, *J .Colloid Interface Sci.,* **1983**, *93*, 140.
5. I. Stan, E. Chifu, Z. Finta and E. Gavrila, *Rev. Roum. Chim.,* **1989**, *34*, 603.
6. I. Stan**,** C.I. Gheorghiu and Z. Kasa, *Studia Univ. Babes-Bolyai, Math.,* **1993**, *38*, 113.
7. E. Chifu, I. Albu, C. I. Gheorghiu, E. Gavrila, M. Salajan and M. Tomoaia-Cotisel, *Rev. Roum. Chim.,* **1986**, *31*, 105.
8. E. Chifu and M. Tomoaia-Cotisel, "Seminars in Biophysics", P. T. Frangopol and V. V. Morariu (Eds), Vol. 4**,** CIP Press, Bucharest, 1987, p. 163-184.
9. M. I. Salajan, A. Mocanu and M. Tomoaia-Cotisel, "Advances in Thermodynamics, Hydrodynamics and Biophysics of Thin Layers", University Press, Cluj-Napoca, 2004, p. 1-117.
10. E. Chifu, I. Stan and M. Tomoaia-Cotisel, *Rev. Roum. Chim*., **2005,** *50*, 297-303.
11. L. Landau and E. Lifschitz, "Mecanique des fluides", 1971**,** Ed. Mir, Moscow.
12. V. G. Levich, "Physicochemical Hydrodynamics", Chap. VIII. Prentice-Hall, Englewood Cliffs, New Jersey, 1962.
13. T. Oroveanu, "Mecanica fluidelor vâscoase", Editura Academiei, 1967, Bucharest.
14. L. E. Scriven, *Chem. Eng. Sci.,* **1960**, *12*, 98.
15. R. Aris, "Vectors, Tensors and the Basic Equations of Fluid Mechanics", Chap. X, Prentice-Hall, Englewood Cliffs, New Jersey, 1962.
16. A. Sanfeld, in "Physical Chemistry Series", W. Jost (Ed.), Vol. I, Acad. Press, New York, 1971, p. 248.
17. I. R. Stan, M. Tomoaia-Cotisel and A. Stan, *Bull. Transilvania Univ. Brasov,* **2006**, *13*, 357-367.
18. A. Wierschem, H. Linde and M. G. Velarde, *Phys. Rev. E.,* **2000**, *62,* 6522.
19. Y. T. Hu and A. Lips, *Phys. Rev. Lett.*, **2003**, *91*, 1.
20. H. A. Stone and L. G. Leal, *J. Fluid Mech.,* **1990**, *220*, 161.
21. W. J. Milliken, H. A. Stone and L. G. Leal, *Phys. Fluids,* A, **1993**, *5*, 69.
22. C. D. Eggleton and K. J. Stebe, *J. Colloid Interface Sci.,* **1998**, *208,* 68.
23. R. Monti, R. Savino and G. Alterio, *Acta Astronautica,* **2002**, *51*, 789.